Scd1 controls de novo beige fat biogenesis through succinate-dependent regulation of mitochondrial complex II

Keli Liu[a,b], Liangyu Lin[a], Qing Li[a], Yueqing Xue[a], Fanjun Zheng[a], Guan Wang[a], Chunxing Zheng[a], Liming Du[a], Mingyuan Hu[a], Yin Huang[a], Changshun Shao[c], Xiangyin Kong[a], Gerry Melino[d], Yufang Shi[a,b,c,1], and Ying Wang[a,1]

[a]CAS Key Laboratory of Tissue Microenvironment and Tumor, Shanghai Institute of Nutrition and Health, Shanghai Institutes for Biological Sciences, University of Chinese Academy of Sciences, Chinese Academy of Sciences, 200031 Shanghai, China; [b]School of Life Science and Technology, ShanghaiTech University, 200031 Shanghai, China; [c]The First Affiliated Hospital of Soochow University, State Key Laboratory of Radiation Medicine and Protection, Institutes for Translational Medicine, Soochow University, 215123 Suzhou, China; [d]Biochemistry Laboratory, Istituto Dermopatico Immacolata (IDI-IRCCS), 00100 Rome, Italy; and [e]Department of Experimental Medicine, University of Rome Tor Vergata, 00133 Rome, Italy

Edited by Tak W. Mak, University Health Network, Toronto, ON, Canada, and approved December 17, 2019 (received for review August 22, 2019)

Preadipocytes can give rise to either white adipocytes or beige adipocytes. Owing to their distinct abilities in nutrient storage and energy expenditure, strategies that specifically promote "beiging" of adipocytes hold great promise for counterbalancing obesity and metabolic diseases. Yet, factors dictating the differentiation fate of adipocyte progenitors remain to be elucidated. We found that stearoyl-coenzyme A desaturase 1 (Scd1)-deficient mice, which resist metabolic stress, possess augmentation in beige adipocytes under basal conditions. Deletion of Scd1 in mature adipocytes expressing Fabp4 or Ucp1 did not affect thermogenesis in mice. Rather, Scd1 deficiency shifted the differentiation fate of preadipocytes from white adipogenesis to beige adipogenesis. Such effects are dependent on succinate accumulation in adipocyte progenitors, which fuels mitochondrial complex II activity. Suppression of mitochondrial complex II by Atpenin A5 or oxaloacetic acid reverted the differentiation potential of Scd1-deficient preadipocytes to white adipocytes. Furthermore, supplementation of succinate was found to increase beige adipocyte differentiation both in vitro and in vivo. Our data reveal an unappreciated role of Scd1 in determining the cell fate of adipocyte progenitors through succinate-dependent regulation of mitochondrial complex II.

stearoyl-coenzyme A desaturase 1 (Scd1) | beige fat biogenesis | preadipocytes | succinate | mitochondrial complex II

From an evolutionary perspective, cells from yeast to man possess lipid droplets as storage of triglycerides for future energy consumption (1). As a specialized tissue, fat bodies first appeared in arthropods (2). In mammals, adipose tissues are for energy storage and caloric intake balance. This adipocyte-composed loose connective tissue also helps cushion and insulate the body (3). Adipose tissue is also integrally involved in various other biological processes such as neuroendocrine and immune regulation (4). According to their molecular characteristics and distinct functions, mammalian adipose tissues can be classified as white adipose tissue (WAT) for energy storage and brown adipose tissue (BAT) for energy dissipation and heat generation (5, 6). Upon chronic cold exposure or exercise, a process termed "beiging" occurs in WAT through generating beige adipocytes and conducts nonshivering thermogenesis by converting nutrients into chemical energy in the form of heat (7, 8). These postnatal induced beige adipocytes share similarities with brown adipocytes, such as multilocular lipid droplets, high levels of uncoupling protein 1 (Ucp1), as well as thermogenic capacity (9–11). Strategies inducing beige adipogenesis hold great promise in counterbalancing overnutrition and metabolic disorders.

The cellular features and functions between beige adipocytes and brown adipocytes are similar; however, their origins are quite different. By employing lineage-tracing mouse models, it has been revealed that progenitors of brown adipocytes reside in the dermomyotome (12). In contrast, beige adipocytes originate from Myf5-negative progenitors, a common cell population that also gives rise to white adipocytes (5). Previous studies have demonstrated that adipose tissue-derived mesenchymal stem cells (ADSCs) located at the perivascular region are the progenitors for de novo beige and white adipogenesis during the development, expansion, or regeneration of adipose tissue (8, 13). ADSCs can differentiate into white or beige adipocytes when cultured in appropriate conditions. By utilizing these in vitro systems, it was found that these well-orchestrated adipogenic processes are controlled by a large number of transcriptional factors such as PRDM16, C/EBPs, PPARγ, and PGC1α, which control distinct stages of adipogenesis (14–16). In the last decade, studies have made a giant leap in understanding the mechanism of adipocyte differentiation. However, few strategies are available to manipulate the fate of ADSCs and increase adaptive thermogenesis.

Lipogenesis and lipolysis are two major coordinated events for adipocytes to maintain energy homeostasis and key factors involved in the regulated formation and function of different adipocyte types (17, 18). Enhanced expression and activity of lipogenic genes

Significance

Adipose tissue-derived mesenchymal stem cells (ADSCs) are well-known in the generation of both white and beige adipocytes and the maintenance of adipose tissue homeostasis. Stearoyl-coenzyme A desaturase 1 (Scd1) is a rate-limiting enzyme for monounsaturated fatty acids. Here, we show that deficiency of Scd1 promotes the formation of beige adipocytes in white adipose tissue by directing de novo beige adipogenesis. In the absence of Scd1, succinate accumulation was enhanced in ADSCs and fueled mitochondrial complex II activities. Notably, we demonstrate that succinate controls the potential of beige adipogenesis of ADSCs both in vitro and in vivo. These findings reveal an unidentified negative regulatory relationship between Scd1 and succinate during adipogenesis, holding great potential for combating obesity.

Author contributions: K.L. designed experiments; K.L. performed experiments; L.L., Q.L., Y.X., F.Z., and G.W. helped conduct experiment; X.K. provided mice; K.L. analyzed data; K.L. prepared the original manuscript; L.L., Q.L., Y.X., M.H., and G.M. assisted in constructing manuscript; C.Z., L.D., and Y.H. made comments and suggestions; Y.W. and Y.S. led the project; and Y.W. and Y.S. wrote the paper.

The authors declare no competing interest.

This article is a PNAS Direct Submission.

[1]To whom correspondence may be addressed. Email: yufangshi@sibs.ac.cn or yingwang@sibs.ac.cn.

This article contains supporting information online at https://www.pnas.org/lookup/suppl/doi:10.1073/pnas.1914553117/-/DCSupplemental.

First published January 17, 2020.

are concomitant with the accumulation of triacylglycerol in adipocytes. Among them, stearoyl-coenzyme A desaturase 1 (Scd1) is the rate-limiting enzyme for catalyzing saturated fatty acids into monounsaturated fatty acids, mainly for the production of oleate and palmitoleate (19). A high level of Scd1 expression is correlated with obesity and some metabolic diseases. Blockade or deficiency of Scd1 in mice inhibited the progression of obesity and insulin resistance induced by a high-fat diet (HFD) (20). Specific knockout of Scd1 in liver or skin can also provide mice with protection against high-carbohydrate- or high-fat diet-induced adiposity through impairment of gluconeogenesis in liver or up-regulation of thermogenic processes (21, 22). Detailed investigations into the biological significance of Scd1 in the metabolism of adipose tissues will provide key insights for understanding the pathophysiological mechanisms of metabolic diseases and exploiting novel therapeutic strategies.

Here, we found that Scd1 deficiency promoted the de novo generation of beige adipocytes, rather than switching white adipocytes into beige adipocytes. The preference of Scd1-deficient ADSCs for beige adipocyte differentiation resulted from increased activity of mitochondrial complex II fueled by accumulated succinate. Succinate alone was sufficient to redirect ADSCs for beige adipogenesis. Taken together, our results demonstrate a key role of Scd1–succinate coupling in dictating adipocyte progenitor cells for beige adipogenesis and adaptive thermogenesis.

Results

Loss of Scd1 Potentiates Beige Adipocyte Formation. Previous studies have reported that Scd1 could be a potential therapeutic target to control obesity and its related metabolic disorders (20). To verify the role of Scd1 in energy metabolism, $Scd1^{ab\text{-}Xyk}$ mice, with a mutation of the *Scd1* gene, were subjected to an HFD to induce obesity (23). Consistently, we found that these mice are resistant to the gains of body weight and fat mass and the development of insulin resistance (Fig. 1*A* and *SI Appendix*, Fig. S1 *A* and *B*). In addition, the loss of Scd1 increased oxygen (O_2) consumption, whole-body carbon dioxide (CO_2) production, and heat generation, when monitored in metabolic cages (Fig. 1*B*).

We further performed histological analysis of the WAT and BAT from these wild-type (WT) mice and $Scd1^{ab\text{-}Xyk}$ mice upon HFD feeding. We found that many more multilocular beige adipocytes were accumulated in inguinal WAT (iWAT) of mice with Scd1 functional deficiency, as analyzed by hematoxylin and eosin (H&E) and Ucp1 staining (Fig. 1*C*). Additionally, genes associated with thermogenesis were much higher in iWAT of Scd1-deficient mice than that of WT mice, verifying that an enhanced formation of beige adipocytes occurs when Scd1 is ablated (Fig. 1*D*). Considering the inherent differences in thermogenesis among distinct inbred mice (24), another strain of Scd1-deficient mice in C57BL/6 background ($Scd1^{tm1Ntam}$) was also tested in the same study. Consistently, Scd1 deficiency ($Scd1^{tm1Ntam}$) also protected mice from HFD-induced obesity and insulin resistance (*SI Appendix*, Fig. S1 *C–F*). Compared with WT mice, Scd1-deficient C57BL/6 mice exhibited higher potentials in energy expenditure and more beige adipocyte formation in iWAT (*SI Appendix*, Fig. S1 *G* and *H*).

To examine whether these enriched beige adipocytes in iWAT of Scd1-deficient mice are preexisting or induced by HFD treatment, we analyzed the tissue mass and morphological features of iWAT of WT and Scd1-deficient mice subjected to a normal diet. As expected, mice with ablation of Scd1 had a significant increase in the mass of interscapular BAT and a lower mass of iWAT (Fig. 1*E*). H&E staining also revealed more extensive multilocular adipocytes distributed in the inguinal fat depots of $Scd1^{ab\text{-}Xyk}$ and $Scd1^{tm1Ntam}$ mice than those of control mice (Fig. 1*F* and *SI Appendix*, Fig. S1*I*). Assays for detecting thermogenesis-associated genes in iWAT showed a significant enhancement in $Scd1^{ab\text{-}Xyk}$ mice compared with controls (Fig. 1*G*). These data show that deletion of Scd1 strengthens beige adipocyte formation and confers mice with resistance to HFD-induced obesity.

Enriched Beige Adipocytes in Scd1-Deficient Mice Are Not Related to the Transition between White and Beige Adipocytes. The accumulation of beige adipocytes in vivo usually requires an external stimulus such as cold or exercise. Therefore, illustrating how Scd1 deficiency dictates beige fat biogenesis under basal conditions or upon HFD feeding may provide new strategies to combat metabolic diseases. Beige adipocytes can be generated by a lineage conversion from mature unilocular adipocytes, a well-known process termed beiging (13, 25–27). To verify whether beige adipocytes in Scd1-deficient mice originate from white adipocytes, *Scd1* was deleted in mature adipocytes by crossing mice bearing *flox* alleles of *Scd1* with $Fabp4^{Cre}$ (fatty acid-binding protein 4) mice, named $F^{Cre}Scd1^{flox}$ (*SI Appendix*, Fig. S2*A*). We proceeded to analyze the inguinal fat mass, adipocyte size, and multilocular lipid droplet appearance in $F^{Cre}Scd1^{flox}$ mice. Distinct from the changes in adipose tissue of $Scd1^{ab\text{-}Xyk}$ and $Scd1^{tm1Ntam}$ mice, a limited difference was observed in mice with Scd1 deficiency in mature adipocytes (Fig. 2 *A* and *B*). Also, these $F^{Cre}Scd1^{flox}$ mice showed comparable or lower levels of thermogenesis-associated genes in BAT as well as in inguinal and gonadal WAT (Fig. 2*C* and *SI Appendix*, Fig. S2*B*). Next, these $F^{Cre}Scd1^{flox}$ mice were fed an HFD. Compared with littermate controls, no changes of body weight, fat and lean mass, insulin resistance, and energy metabolism including O_2 consumption, CO_2 production, and heat generation were observed in $F^{Cre}Scd1^{flox}$ mice (Fig. 2 *D–G* and *SI Appendix*, Fig. S2*C*).

Beige adipocytes have high plasticity, which can regain the phenotypes and functions of white adipocytes, especially upon HFD feeding (28). We questioned whether the sustained "whitening process" is affected in Scd1-deficient mice. Thus, we constructed mice with an Scd1-specific deletion in Ucp1-positive cells (named $U^{Cre}Scd1^{flox}$) (*SI Appendix*, Fig. S2*D*). However, no difference was shown in body weight and rectal temperature between $U^{Cre}Scd1^{flox}$ mice and their littermate controls (*SI Appendix*, Fig. S2*E*). Also, $U^{Cre}Scd1^{flox}$ mice showed similar adipocyte size in iWAT and BAT to that of control mice (*SI Appendix*, Fig. S2*F*). When fed an HFD, $U^{Cre}Scd1^{flox}$ and control mice gained body weight in a similar pattern (Fig. 2*H*). Monitored by using metabolic cages, these $U^{Cre}Scd1^{flox}$ mice and control mice exhibited comparable levels in O_2 consumption, CO_2 production, and heat generation in both light and dark cycles (Fig. 2*I* and *SI Appendix*, Fig. S2*G*). Meanwhile, the size and morphology of adipocytes in iWAT, gonadal WAT (gWAT), and BAT were not affected by Scd1 deficiency in beige/brown adipose tissue (Fig. 2*J*). In summary, loss of Scd1 does not regulate the transition between white and beige adipocytes.

Scd1 Dictates the Developmental Fate of Adipocyte Progenitors. We thus far have excluded the possibility that the accumulation of beige adipocytes in mice with Scd1 deficiency was initiated by the conversion of mature white adipocytes. We further checked an alternative possibility that beige adipocytes can be more vigorously generated from precursors when Scd1 is deficient. To achieve this, ADSCs were isolated from iWAT of WT and $Scd1^{tm1Ntam}$ mice. These cells were featured as $CD45^{-}CD31^{-}Sca\text{-}1^{+}CD140a^{+}$ (*SI Appendix*, Fig. S3*A*). ADSCs derived from WT and $Scd1^{tm1Ntam}$ mice showed comparable levels in the expression of CD137 and TBX1, markers for the recognition of beige adipocyte progenitors (9) (*SI Appendix*, Fig. S3*B*). Also, we found that the expression of *Prdm16*, *Pgc1a*, *Cebpa*, *Cebpb*, *Cebpd*, and *Srebf1* in both WT and Scd1-deficient ADSCs exhibited limited differences (*SI Appendix*, Fig. S3*C*).

Given that ADSCs can undergo white and beige adipogenesis in certain culture conditions, cells from WT and Scd1-deficient mice were examined for their differentiation ability. These ADSCs

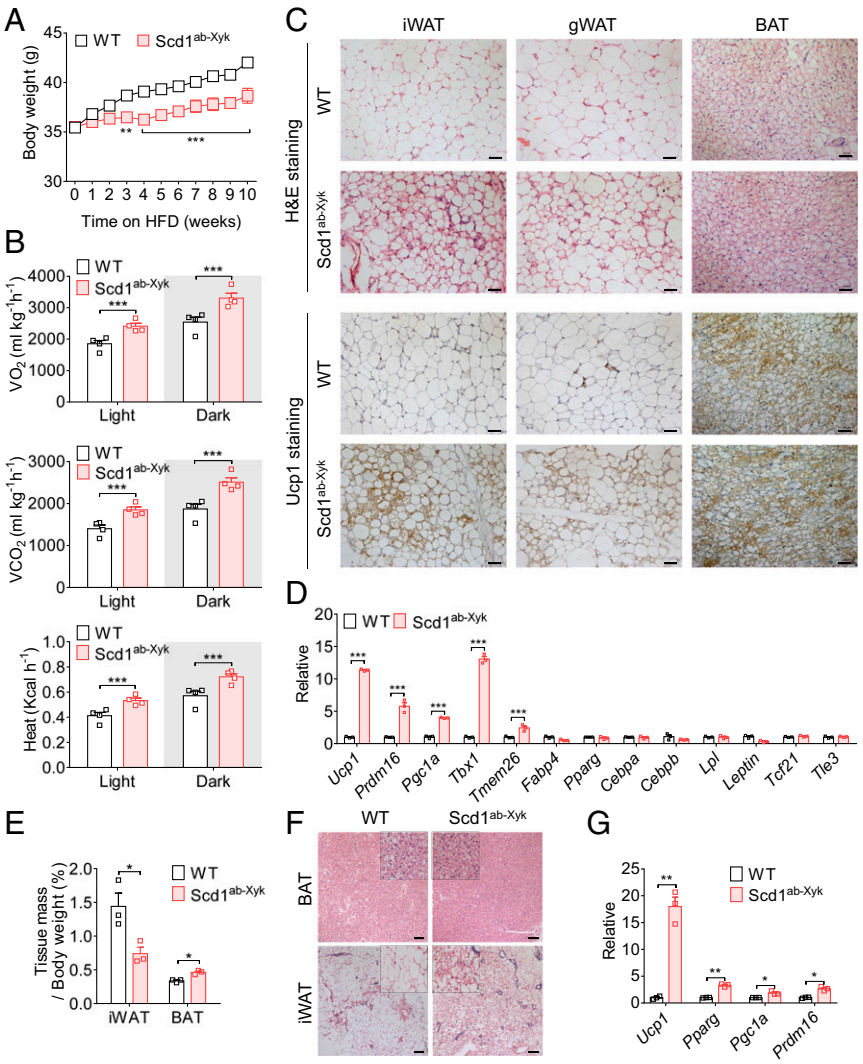

Fig. 1. Loss of Scd1 potentiates beige adipocyte formation. (*A*) Body weight of WT and Scd1 mutant (Scd1$^{ab\text{-}Xyk}$) mice fed an HFD for 10 wk ($n = 5$ for each group, repeated three times). (*B*) Daily O_2 consumption, CO_2 production, and heat generation of WT and Scd1 mutant (Scd1$^{ab\text{-}Xyk}$) mice fed an HFD ($n \geq 3$ for each group, repeated two times). (*C*) Representative H&E staining and immunohistological staining for Ucp1 in inguinal WAT, gonadal WAT, and interscapular BAT of WT and Scd1 mutant (Scd1$^{ab\text{-}Xyk}$) mice fed an HFD. (Scale bars, 50 μm.) (*D*) Relative mRNA levels of thermogenic and adipogenic genes in iWAT of WT and Scd1 mutant (Scd1$^{ab\text{-}Xyk}$) mice fed an HFD ($n = 3$ for each group, repeated three times). (*E*) The ratio of tissue mass (iWAT or BAT) to body weight in WT and Scd1 mutant (Scd1$^{ab\text{-}Xyk}$) mice (8 wk old; $n = 3$ for each group, repeated three times). (*F*) H&E staining of representative sections of iWAT and BAT from WT and Scd1 mutant (Scd1$^{ab\text{-}Xyk}$) mice (8 wk old). (Scale bars, 100 μm.) (*G*) Relative expression levels of *Ucp1*, *Pparg*, *Pgc1a*, and *Prdm16* in iWAT from WT and Scd1 mutant (Scd1$^{ab\text{-}Xyk}$) mice (8 wk old; $n = 3$ for each group, repeated three times). Data are shown as mean ± SEM. $^*P < 0.05$, $^{**}P < 0.01$, and $^{***}P < 0.001$.

were initiated in beige adipogenic culture, and we found adipocytes generated from WT and Scd1-deficient ADSCs exhibited similar multilocular morphology and mRNA levels in thermogenic and adipogenic genes (*SI Appendix*, Fig. S3 *D* and *E*). Surprisingly, when we cultured these ADSCs in white adipogenic differentiation medium, which contains no chemical or hormonal inducer of beige adipogenesis, ADSCs from Scd1-deficient mice were still converted into beige adipocytes. As predicted, adipocytes generated from Scd1-deficient ADSCs showed more multilocular morphology and smaller lipid droplets compared with those from WT ADSCs (Fig. 3 *A* and *B*). No difference was found in the expression of genes associated with white adipogenesis, including *Cebpa*, *Cebpb*, *Pparg*, *Fabp4*, and *Leptin* (Fig. 3*C*). However, we observed a robust enhancement of mRNAs encoding key thermogenic genes in differentiated ADSCs with Scd1 deficiency, including *Ucp1*, *Prdm16*, *Pgc1a*, *Cidea*, *Cox8b*, and *Srebf1* (Fig. 3*C*). Similar results were shown in protein levels of Lipin1, Ucp1, PGC1α, and C/EBPβ (Fig. 3*D*). Taken together, loss of function of Scd1 in ADSCs determines cells with a preference for beige adipocyte generation in response to signals for classical white adipogenesis.

To verify the regulatory effect of Scd1 in determining the cell fate of adipocyte progenitors in vivo, we conditionally deleted Scd1 in mesenchymal progenitors by crossing Scd1^{flox} mice with Dermo1^{Cre} (also called Twist2^{Cre}) mice (named D^{Cre}Scd1^{flox}) (*SI Appendix*, Fig. S3*F*). Despite the fat mass and the lean mass not being affected by Scd1 deficiency in adipocyte progenitors, more multilocular adipocytes were observed in the iWAT of D^{Cre}Scd1^{flox} mice (Fig. 3 *E* and *F*). Consistently, analysis of genes associated with white or beige adipocyte generation further demonstrated that Scd1 deficiency in adipocyte progenitors facilitates beige adipocyte formation in iWAT (Fig. 3*G*). When these mice were fed an HFD, we found that D^{Cre}Scd1^{flox} mice are resistant to accelerated gain of body weight (Fig. 3*H*). The glucose tolerance, O_2 consumption, and CO_2 production were also significantly

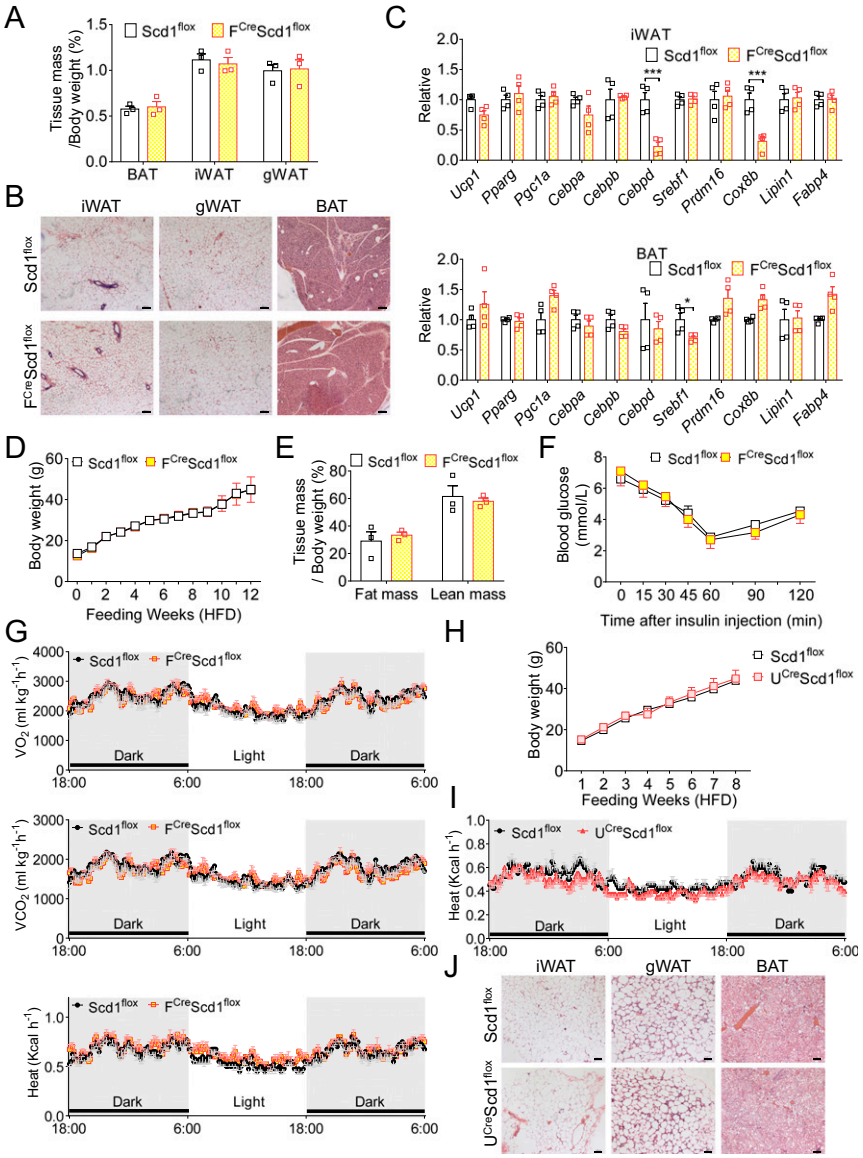

Fig. 2. Enhanced beige adipocytes in the adipose tissue of Scd1-deficient mice is not related to white-to-beige transition. (*A*) The ratio of tissue mass (BAT, iWAT, and gWAT) to body weight of 8-wk-old control ($Scd1^{flox}$) and $F^{Cre}Scd1^{flox}$ mice ($n = 3$ for each group, repeated two times). (*B*) H&E staining of representative sections of iWAT, gWAT, and BAT from 8-wk-old control ($Scd1^{flox}$) and $F^{Cre}Scd1^{flox}$ mice. (Scale bars, 100 μm.) (*C*) Relative mRNA levels of thermogenesis- and adipogenesis-related genes in iWAT and BAT of control ($Scd1^{flox}$) and $F^{Cre}Scd1^{flox}$ mice ($n = 4$ for each group, repeated two times). (*D*) Body weight of control ($Scd1^{flox}$) and $F^{Cre}Scd1^{flox}$ mice fed an HFD for 12 wk ($n \geq 4$ for each group, repeated three times). (*E* and *F*) The ratio of fat mass and lean mass to body weight (*E*) and insulin sensitivity (*F*) of control ($Scd1^{flox}$) and $F^{Cre}Scd1^{flox}$ mice fed an HFD for 12 wk ($n = 3$ for each group, repeated three times). (*G*) Daily O_2 consumption, CO_2 production, and heat production of control ($Scd1^{flox}$) and $F^{Cre}Scd1^{flox}$ mice fed an HFD ($n = 4$ for each group, repeated two times). (*H*) Body weight of control ($Scd1^{flox}$) and $U^{Cre}Scd1^{flox}$ mice fed an HFD for 8 wk ($n \geq 4$ for each group, repeated three times). (*I*) Heat generation of the light cycle and the dark cycle in control ($Scd1^{flox}$) and $U^{Cre}Scd1^{flox}$ mice fed an HFD ($n = 4$ for each group, repeated two times). (*J*) H&E staining of representative sections of iWAT, gWAT, and BAT of control ($Scd1^{flox}$) and $U^{Cre}Scd1^{flox}$ mice fed an HFD for 8 wk. (Scale bars, 100 μm.) Data are shown as mean ± SEM. $^{*}P < 0.05$ and $^{***}P < 0.001$.

improved in $D^{Cre}Scd1^{flox}$ mice compared with that of controls (Fig. 3*I* and *SI Appendix*, Fig. S3*G*). Together, our data provide evidence that deficiency of Scd1 potentiates adipocyte progenitors to undergo beige adipogenesis.

Robust Mitochondrial Complex II Activity in Scd1-Deficient ADSCs Dictates Their Preference for Beige Adipogenesis. As enriched expression of Ucp1 in adipocytes is a mark for high thermogenic ability, we further evaluated the spare respiratory capacity (SRC) in adipocytes derived from WT and Scd1-deficient ADSCs by employing the seahorse XF24 analyzer to measure oxygen consumption rate (OCR). Much higher maximal OCR and extra capacity for energy generation were found in adipocytes differentiated from Scd1-deficient ADSCs, compared with that of WT ADSCs (Fig. 4*A* and *SI Appendix*, Fig. S4*A*). It is well-known that the oxidative phosphorylation (OXPHOS) process is carried out by the electronic transport chain (ETC) composed of a series of complexes on the mitochondrial inner membrane (29). We further detected the quantity and enzymatic activity of mitochondrial complexes. When Scd1 was deficient, no changes were found in the protein levels of these five mitochondrial complexes in either ADSCs or their differentiated adipocytes (Fig. 4*B*). We further examined if the activities of mitochondrial complexes were affected and responsible for the enhanced SRC. As expected, adipocytes derived from Scd1-deficient ADSCs showed

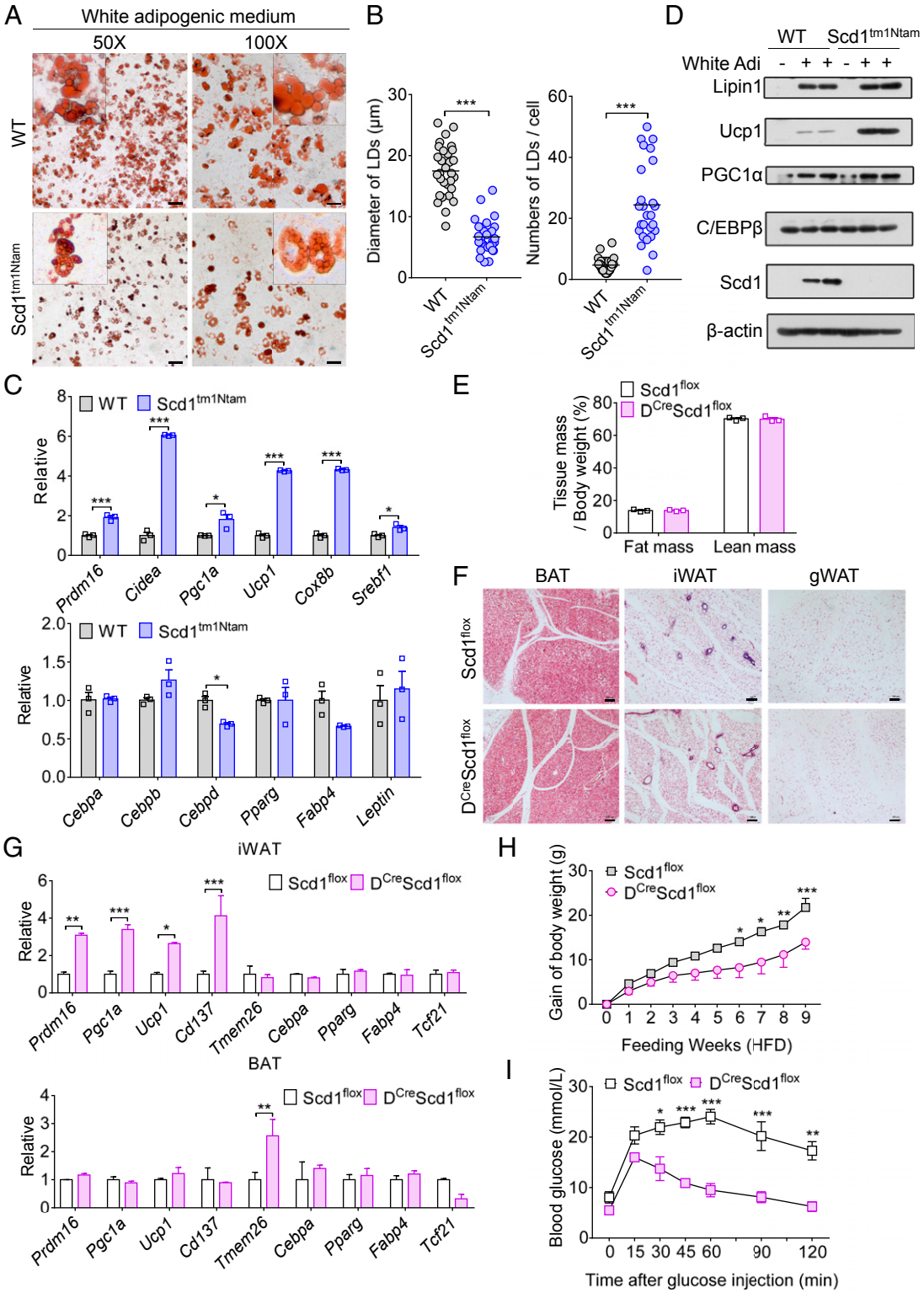

Fig. 3. Scd1 deficiency in ADSCs promotes beige adipogenesis. (*A*) Oil red-O staining of adipocytes generated from WT and Scd1-deficient ($Scd1^{tm1Ntam}$) ADSCs cultured in white adipogenic medium for 7 d. (Scale bars, 100 μm [50×] and 50 μm [100×].) (*B*) The average diameter and numbers of lipid droplets (LDs) per cell in differentiated adipocytes from WT and Scd1-deficient ($Scd1^{tm1Ntam}$) ADSCs cultured in white adipogenic medium ($n = 30$ for each group, repeated three times). (*C*) Relative expression levels of genes associated with thermogenesis (*Top*) and adipogenesis (*Bottom*) in differentiated adipocytes from WT and Scd1-deficient ($Scd1^{tm1Ntam}$) ADSCs cultured in white adipogenic medium ($n = 3$ for each group, repeated three times). (*D*) Immunoblot analysis of Lipin1, Ucp1, PGC1α, C/EBPβ, Scd1, and β-actin in WT and Scd1-deficient ($Scd1^{tm1Ntam}$) ADSCs and their differentiated adipocytes. White Adi, white adipogenic medium. (*E*) The ratio of fat mass and lean mass to body weight in control ($Scd1^{flox}$) and $D^{Cre}Scd1^{flox}$ mice (8 wk old; $n = 3$ for each group). (*F*) H&E staining of representative sections of iWAT, gWAT, and BAT from 8-wk-old control ($Scd1^{flox}$) and $D^{Cre}Scd1^{flox}$ mice. (Scale bars, 100 μm.) (*G*) Relative expression levels of genes associated with white or beige adipocytes in iWAT and BAT from control ($Scd1^{flox}$) and $D^{Cre}Scd1^{flox}$ mice (8 wk old; $n = 3$ for each group). (*H*) Gain of body weight of control ($Scd1^{flox}$) and $D^{Cre}Scd1^{flox}$ mice fed an HFD for 9 wk ($n = 3$ for each group, repeated two times). (*I*) Blood glucose after injection of glucose in control ($Scd1^{flox}$) and $D^{Cre}Scd1^{flox}$ mice fed an HFD for 8 wk ($n = 3$ for each group). Data are shown as mean ± SEM. $^*P < 0.05$, $^{**}P < 0.01$, and $^{***}P < 0.001$.

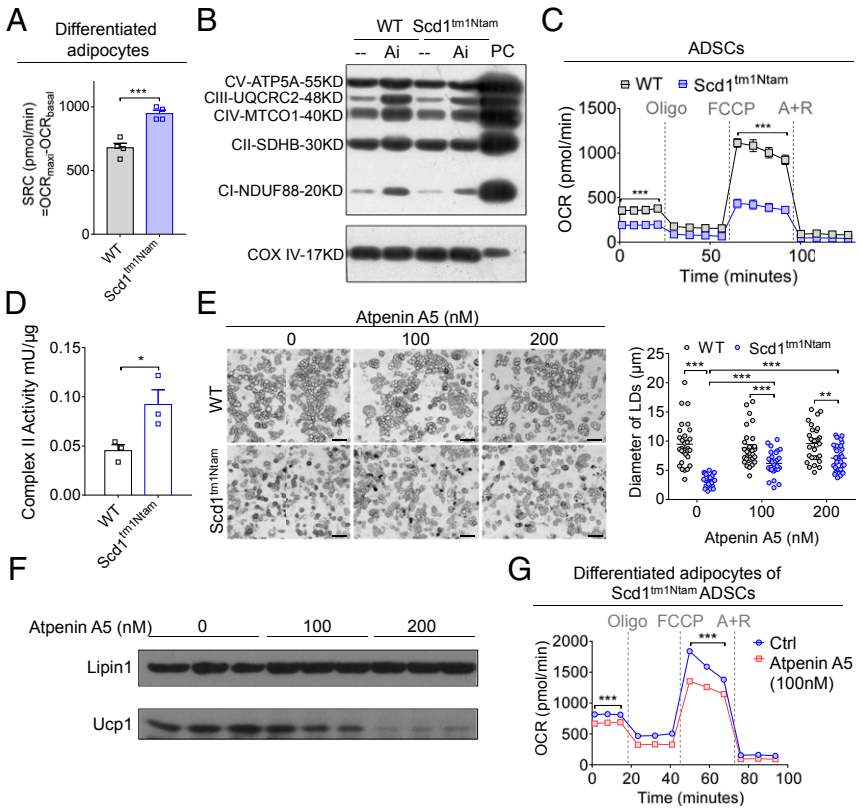

Fig. 4. Enhanced activity of mitochondrial complex II controls Scd1-deficient ADSCs with a propensity for beige adipogenesis. (*A*) Spare respiratory capacity (indicated by the difference between maximal OCR and basal OCR) in differentiated adipocytes from WT and Scd1-deficient (Scd1^{tm1Ntam}) ADSCs cultured in a 24-well plate with white adipogenic medium for 5 d ($n = 4$ for each group, repeated two times). (*B*) Immunoblot analysis of mitochondrial complexes and COXIV in ADSCs derived from WT and Scd1-deficient (Scd1^{tm1Ntam}) mice and their differentiated adipocytes. Ai, adipocytes derived from ADSCs cultured in white adipogenic medium; PC, positive control. (*C*) The OCR in ADSCs from WT and Scd1-deficient (Scd1^{tm1Ntam}) mice. A+R, antimycin and rotenone; Oligo, oligomycin; FCCP, *p*-trifluoromethoxyphenylhydrazone ($n \geq 3$ for each group, repeated three times). (*D*) The activities of complex II per μg of mitochondrial protein in ADSCs derived from WT and Scd1-deficient (Scd1^{tm1Ntam}) mice ($n = 3$ for each group, repeated three times). (*E*) Representative images (*Left*) and the average diameter of lipid droplets (*Right*) of adipocytes differentiated from WT and Scd1-deficient (Scd1^{tm1Ntam}) ADSCs, with Atpenin A5 treatment at concentrations of 0, 100, and 200 nM ($n = 30$ for each group, repeated three times). (Scale bars, 100 μm.) (*F*) Immunoblot analysis of Ucp1 and Lipin1 in adipocytes differentiated from Scd1-deficient (Scd1^{tm1Ntam}) ADSCs, with Atpenin A5 treatment (0, 100, and 200 nM). (*G*) The OCR of adipocytes differentiated from Scd1-deficient (Scd1^{tm1Ntam}) ADSCs, with or without (Ctrl) Atpenin A5 (100 nM) treatment ($n = 3$ for each group). Data are shown as mean ± SEM. $^*P < 0.05$, $^{**}P < 0.01$, and $^{***}P < 0.001$.

an up-regulation in the activities of mitochondrial complexes I, II, and III, with a slightly down-regulation in mitochondrial complex V activity (*SI Appendix*, Fig. S4*B*). Distinct from the enhanced levels of maximal OCR in adipocytes derived from Scd1-deficient ADSCs (*SI Appendix*, Fig. S4*A*), we surprisingly found that ADSCs with Scd1 deficiency exhibit much lower capabilities in OCR and maximal respiratory rate (Fig. 4*C*). However, the activity of mitochondrial complex II was strikingly higher in Scd1-deficient ADSCs than that of WT ADSCs (Fig. 4*D* and *SI Appendix*, Fig. S4*C*).

Mitochondrial complex II is also referred to as succinate dehydrogenase, a unique enzyme that participates in both the tricarboxylic acid (TCA) cycle and ETC. It catalyzes succinate oxidation into fumarate coupled with the reduction of ubiquinone to ubiquinol. To parse out if enhanced activity of mitochondrial complex II in Scd1-deficient ADSCs is responsible for the commitment of beige adipocytes, Atpenin A5, a mitochondrial complex II inhibitor that competitively binds to ubiquinone, was added to ADSCs cultured in white adipogenic differentiation medium. We found that Atpenin A5 significantly increased the sizes of lipid droplets in adipocytes generated from Scd1-deficient ADSCs, and these effects were found to be dose-dependent (Fig. 4*E*). Also, Atpenin A5 down-regulated the mRNA levels of *Ucp1*, *Pgc1a*, *Prdm16*, and *Cox8b*, as well as the protein level of Ucp1 in differentiated ADSCs with Scd1 deficiency (Fig. 4*F* and *SI Appendix*, Fig. S4*D*). No change was detected in the genes for white adipogenesis (*SI Appendix*, Fig. S4*D*). By employing the seahorse XF24 analyzer, we found that Atpenin A5 treatment significantly inhibited the maximal respiratory rate in adipocytes derived from ADSCs with Scd1 deficiency (Fig. 4*G*). Alternatively, oxaloacetate (OAA) was also used to suppress the oxidation of succinate. Similar to the treatment with Atpenin A5, addition of OAA significantly decreased the mRNA levels of *Ucp1*, *Pgc1a*, *Prdm16*, *Cidea*, and *Cox8b* in adipocytes generated from Scd1-deficient ADSCs (*SI Appendix*, Fig. S4*E*). These data strongly suggest that the enhanced activity of mitochondrial complex II in Scd1-deficient ADSCs dictates their preference for beige adipocyte differentiation.

Enriched Succinate in Scd1-Deficient ADSCs Fuels the Activities of Mitochondrial Complex II. We next explored the mechanisms of the increased activity of mitochondrial complex II in ADSCs impacted by Scd1 deficiency. We used liquid chromatography-mass spectrometry (LC-MS) to profile comprehensive metabolites in WT and Scd1-deficient ADSCs and their differentiated adipocytes (Dataset S1). Principal component analysis (PCA) and unsupervised hierarchical clustering showed that WT and Scd1-deficient ADSCs were located at a relative distance (Fig. 5 *A* and *B*). The changes reached the maximum upon stimulation with adipogenic medium in adipocytes generated from WT and Scd1-deficient ADSCs (Fig. 5 *A* and *B*). Thus, a total of 250

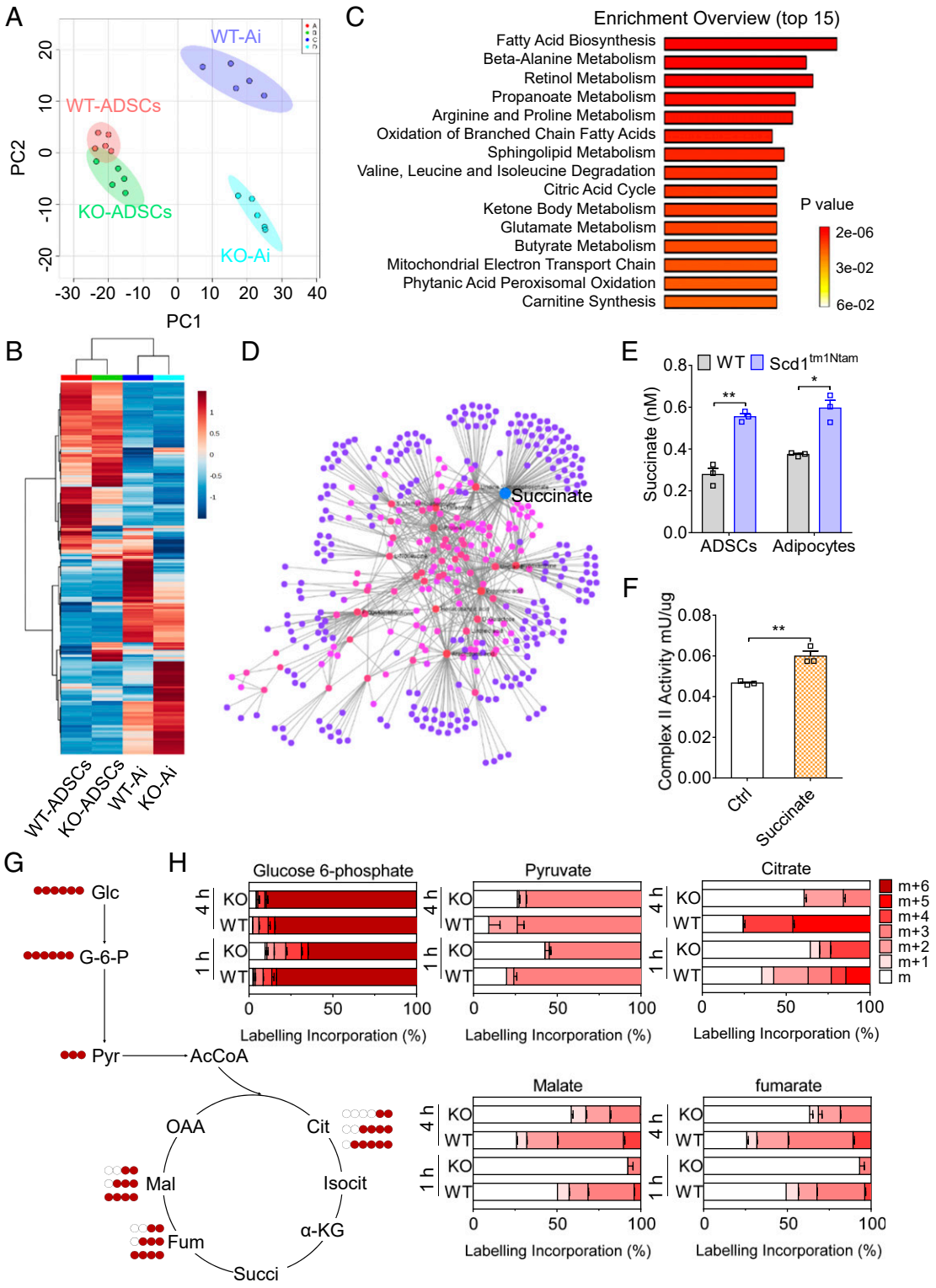

Fig. 5. Accumulated succinate fuels mitochondrial complex II activity in Scd1-deficient ADSCs. (*A* and *B*) Principal component analysis (*A*) and unsupervised hierarchical clustering (*B*) in ADSCs (WT-ADSCs and knockout [KO]-ADSCs, indicated by red and green) and their differentiated adipocytes (WT-Ai and KO-Ai, indicated by purple and blue) from WT and Scd1-deficient (Scd1^{tm1Ntam}) mice ($n = 5$ for each group). (*C*) The analysis of the top 15 most enriched metabolic pathways with a total of 250 metabolites contributing to PC2 by using online tools from MetaboAnalyst. (*D*) Module shown for the network associating the key signature metabolites among WT and Scd1-deficient (Scd1^{tm1Ntam}) ADSCs and their differentiated adipocytes. Edges indicate the experimentally verified interactions among metabolites. The size of nodes indicates betweenness value. (*E*) The concentration of succinate in WT and Scd1-deficient (Scd1^{tm1Ntam}) ADSCs and their differentiated adipocytes cultured in white adipogenic medium for 7 d ($n = 3$ for each group, repeated two times). (*F*) The activity of mitochondrial complex II in adipocytes generated from WT ADSCs with (succinate; 2 mM) or without (Ctrl) succinate stimulation ($n = 3$ for each group, repeated two times). (*G*) Schematic illustration of ^{13}C tracing of [U-^{13}C]glucose in glycolysis and the TCA cycle. (*H*) Adipocytes generated from WT and Scd1-deficient (Scd1^{tm1Ntam}, KO) ADSCs were incubated with [U-^{13}C]glucose for 1 or 4 h. After extracting polar metabolites, the labeling proportion of each isotopologue in the total was calculated ($n = 5$ for each group). Data are presented as mean ± SEM. *$P < 0.05$ and **$P < 0.01$.

metabolites loading for PC2 were analyzed for the enrichment analysis. We found that these detectable metabolites were mainly associated with fatty acid metabolism and oxidation, amino acid metabolism and degeneration, the citric acid cycle, as well as the electronic transport chain (Fig. 5*C*). We next depicted metabolite differences using a network-based permutation test. These 250 metabolites were analyzed and mapped to the selected molecular interaction network to create subnetworks. Among them, succinate showed the highest betweenness centrality value (Fig. 5*D* and Dataset S2). We further confirmed the elevated concentration of succinate in ADSCs derived from $Scd1^{tm1Ntam}$ mice and their descendants during white adipogenesis, relative to those of control cells (Fig. 5*E*). Indeed, addition of cell-permeable diethyl succinate (hereafter referred to as succinate) to ADSCs can significantly increase the activity of mitochondrial complex II (Fig. 5*F*). Therefore, succinate accumulation in Scd1-deficient ADSCs is associated with their enhanced activity of mitochondrial complex II.

Based on the analysis that the most relevant metabolic pathway affected by Scd1 deficiency is fatty acid metabolism, we asked if the accumulated fatty acids catabolized by Scd1 were related to the enhanced succinate in Scd1-deficient ADSCs. We profiled major fatty acids in white adipose tissue of WT and $Scd1^{ab\text{-}Xyk}$ mice and found that loss of Scd1 induced a lower ratio of monounsaturated fatty acids (C16:1 and C18:1) to saturated fatty acids (C16:0 and C18:0) (*SI Appendix*, Fig. S5 *A* and *B*). Therefore, we supplemented oleic acid, a monounsaturated fatty acid, to Scd1-deficient ADSCs under white adipogenic conditions. By monitoring cell morphology, we found that the tendency of Scd1-deficient ADSCs to generate beige adipocytes was significantly impaired by this oleic acid treatment (*SI Appendix*, Fig. S5*C*). More importantly, addition of oleic acid sharply decreased the concentration of succinate and the activity of mitochondrial complex II in adipocytes generated from Scd1-deficient ADSCs (*SI Appendix*, Fig. S5 *D* and *E*). Also, the expression of beige adipogenic genes in these adipocytes differentiated from Scd1-deficient ADSCs was inhibited by oleic acid (*SI Appendix*, Fig. S5*F*). Thus, the absence of monounsaturated fatty acids endows ADSCs with a tendency to differentiate into beige adipocytes via succinate.

To gain insights into the impact of Scd1 deficiency on succinate accumulation, we used isotope-labeled glucose and glutamate as carbon tracers for metabolic flux analysis. ADSCs from WT and Scd1-deficient mice were cultured under white adipogenic conditions for 10 d and then incubated with [U-^{13}C]glucose or [U-^{13}C] glutamate. We found an impaired incorporation of ^{13}C carbons from [U-^{13}C]glucose into glycolysis and the TCA cycle in Scd1-deficient adipocytes (Fig. 5 *G* and *H*). However, a significant proportion of ^{13}C carbons from [U-^{13}C]glutamate was incorporated into the GABA shuttle and TCA cycle in these Scd1-deficient adipocytes (*SI Appendix*, Fig. S5 *G* and *H*). These results suggest that Scd1 deficiency in differentiated adipocytes endows them with a preference to consume glutamate rather than glucose, subsequently resulting in succinate accumulation.

Succinate Stimulates Beige Adipogenesis. To investigate whether succinate directly regulates the beige adipogenesis process, succinate was used to treat ADSCs under the white adipocyte differentiation condition. With succinate treatment, ADSCs exhibited more significant accumulation of multiloculated lipid droplets and up-regulation of thermogenic gene expression compared with those of control ADSCs (*SI Appendix*, Fig. S6 *A* and *B*). These results reveal that succinate endows ADSCs with a preference for the generation of beige adipocytes. In addition, succinate treatment was found to increase the maximal respiratory capacity of ADSCs in a dose-dependent manner (Fig. 6*A*). Such amplified maximal OCR in succinate-treated ADSCs can be reversed by Atpenin A5 treatment, an inhibitor of mitochondrial complex II (*SI Appendix*, Fig. S6*C*). RNA-sequencing analysis showed a clear distinction between adipocytes generated from ADSCs that were treated with (Suc-Adi) and those without succinate (Ctrl-Adi). Compared with Ctrl-Adi, Suc-Adi are enriched with genes associated with beige adipocytes, although less in the representative genes related to white adipocytes (Fig. 6*B*) (30–32). Accordingly, pathway enrichment analysis demonstrated that the PI3K-Akt pathway and the AMPK pathway were altered in adipocytes differentiated from ADSCs with succinate treatment, further supporting succinate-treated ADSCs with a strong preference to generate beige adipocytes (*SI Appendix*, Fig. S6 *D* and *E*).

Given that succinate in metabolic pathways is important for reactive oxygen species (ROS) production, we next questioned if succinate oxidation was involved in promoting beige differentiation. We first measured ROS generation in mitochondria and found that a much higher level of ROS can be observed in adipocytes differentiated from Scd1-deficient ADSCs, compared with adipocytes from WT ADSCs (*SI Appendix*, Fig. S7*A*). Also, addition of succinate resulted in a rapid and robust enhancement of ROS formation in mitochondria of WT and Scd1-deficient adipocytes, strongly suggesting that succinate is a potent driver of ROS generation during adipogenesis (*SI Appendix*, Fig. S7*B*). Of note, supplementation of mitoquinone, a mitochondrial ROS scavenger, could significantly suppress the beige adipogenesis induced by succinate treatment (*SI Appendix*, Fig. S7 *C* and *D*). These data show that mitochondrial ROS induced by succinate can be associated with the regulation of Scd1 in beige adipogenesis.

We next tested if the enhanced beige adipogenesis by succinate can be seen in in vivo experiments. First, we employed a de novo adipogenesis system. ADSCs were isolated from Fabp4-mTmG reporter mice generated by crossing $Fabp4^{Cre}$ mice with mTmG mice (Fig. 6*C*) (33). These cells were mixed with Matrigel and subcutaneously injected into the chest of mice. Mice were exposed to succinate in drinking water at different concentrations (5 and 10 mM) for 4 wk. The Matrigel plugs were isolated and counted for these mT/mG-labeled multilocular adipocytes. More beige adipocytes were observed in the succinate-treated group (Fig. 6 *D*–*F*). Consistently, succinate amplified Ucp1 expression in adipocytes in the Matrigel plugs (Fig. 6 *E* and *F* and *SI Appendix*, Fig. S8*A*). Also, mRNA expression of beige adipogenic genes, including *Ucp1*, *Cox8b*, and *Pgc1a*, was also elevated (Fig. 6*F*).

To further evaluate the effects of succinate in controlling beige adipocyte formation in vivo, we detected the metabolic parameters in mice treated with succinate. Succinate administration did not influence body weight, tissue mass (iWAT, gWAT, and BAT), and histology of other nonfat organs including kidney, lung, spleen, and liver (*SI Appendix*, Fig. S8 *B*–*D*). Of note, the formation of beige adipocytes in WAT was enhanced in mice with succinate administration, compared with that of the control group (*SI Appendix*, Fig. S8*D*). Elevated mRNA levels of thermogenic genes in both iWAT and gWAT also verified the promoting effects of succinate in beige adipogenesis (*SI Appendix*, Fig. S8*E*). More importantly, when succinate was supplemented in drinking water for HFD-fed mice, gains in body weight and fat mass were suppressed (Fig. 6 *G* and *H*). Many more beige adipocytes were observed in the adipose tissue of succinate-treated obese mice (Fig. 6*I*). Consistently, these succinate-treated mice also showed enhanced whole-body energy expenditure (Fig. 6*J*). Taken together, these results suggest that succinate administration dramatically induces beige adipogenesis.

Discussion

Comprehending the development and maintenance of beige adipogenesis helps develop strategies to fight obesity. In the present study, we identified Scd1 as a key enzyme in controlling beige adipogenesis. Its deficiency in ADSCs conferred cells with the ability to differentiate into beige adipocytes. Detailed analysis revealed that an accumulation of succinate induced by Scd1 deficiency enhances the activity of mitochondrial complex II and promotes ADSCs to differentiate into beige adipocytes.

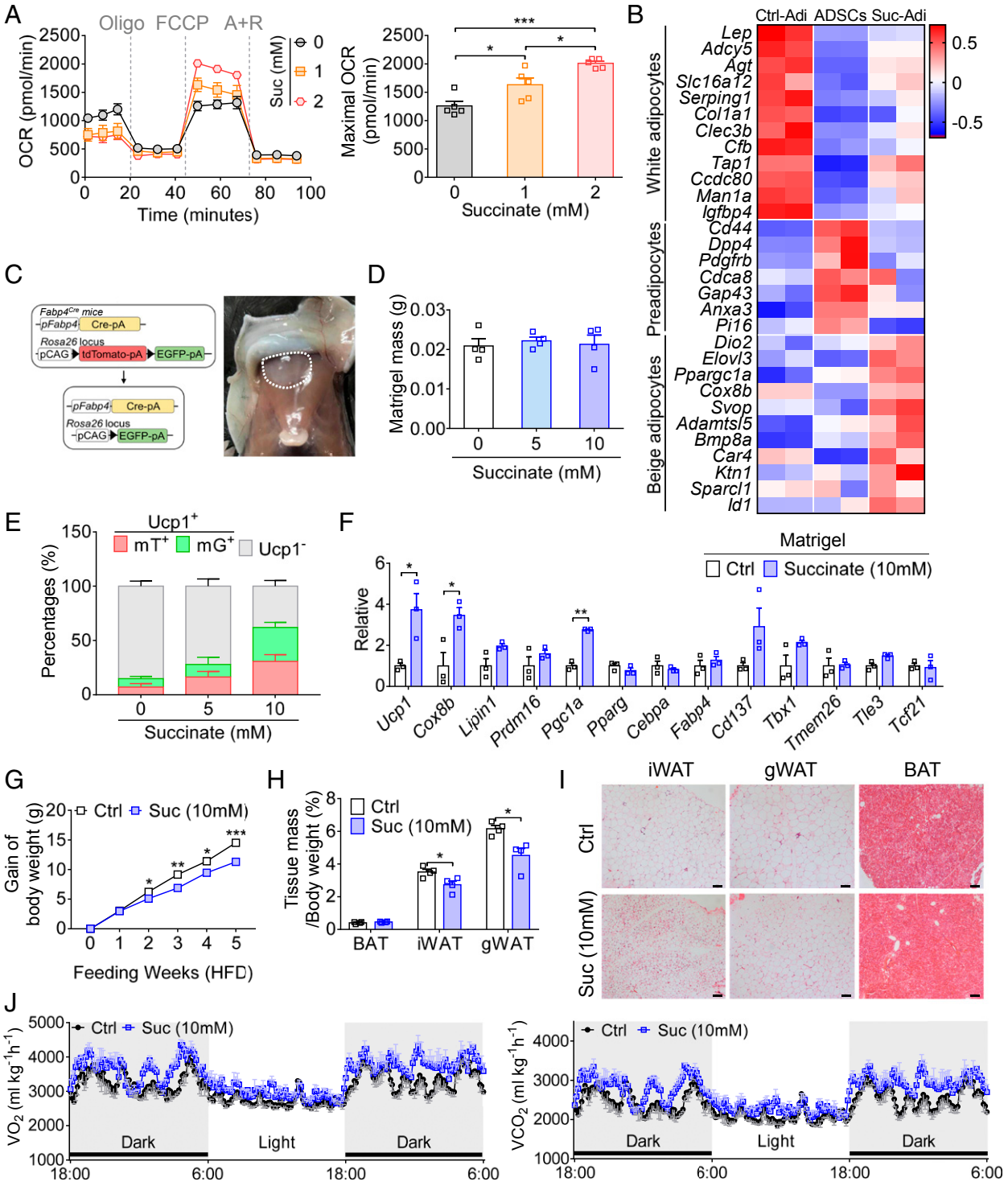

Fig. 6. Succinate promotes beige adipogenesis. (*A*) The OCR (*Left*) and the maximal OCR (*Right*) of adipocytes differentiated from WT ADSCs, with or without succinate (Suc; 1 and 2 mM) treatment ($n = 5$ for each group). (*B*) Heatmap showing expression profiles of select genes in each group. Ctrl-Adi, differentiated adipocytes; Suc-Adi, succinate-treated differentiated adipocytes. The color scale shows normalized fragments per kilobase million representing the mRNA level of each gene in blue (low expression) to white to red (high expression) scheme. (*C*) Schematic representation for generation of Fabp4^{Cre}; mTmG mice by crossing mTmG mice with Fabp4^{Cre} mice (*Left*); representative image of a mouse injected with a mixture of Matrigel and ADSCs (*Right*). The white dashed line indicates the Matrigel implant. (*D*) Mass of Matrigel mixed with ADSCs implanted in mice, with or without succinate (5 and 10 mM) administration in drinking water for 4 wk ($n = 4$ for each group, repeated two times). (*E*) The percentages of Ucp1$^+$ adipocytes with tdTomato (mT$^+$) or EGFP (mG$^+$) and Ucp1$^-$ adipocytes in fluorescence-labeled adipocytes ($n \geq 9$ for each group, repeated two times). (*F*) Relative expression of genes associated with thermogenesis and adipogenesis in implants with or without succinate treatment (10 mM) ($n = 3$ for each group, repeated two times). (*G*) Gains of body weight of WT mice fed an HFD for 5 wk with or without succinate (10 mM) in drinking water ($n = 4$ for each group). (*H*) The ratio of tissue mass (BAT, iWAT, and gWAT) to body weight in WT mice fed an HFD for 5 wk with or without succinate (10 mM) in drinking water ($n = 4$ for each group). (*I*) H&E staining of representative sections of iWAT, gWAT, and BAT from obese mice with or without succinate (10 mM) supplementation. (Scale bars, 100 μm.) (*J*) Daily O_2 consumption and CO_2 production of obese mice supplied with or without succinate (10 mM) treatment ($n = 4$ for each group). Data are shown as mean ± SEM. $^*P < 0.05$, $^{**}P < 0.01$, and $^{***}P < 0.001$.

Such regulation can be reversed by the addition of oleic acid. Notably, administration of succinate alone could accelerate beige adipogenesis through strengthening the activity of mitochondrial complex II.

In this study, we also analyzed the negative role of Scd1 in beige adipogenesis during HFD feeding-induced adiposity, providing potential strategies to combat obesity. We found that ablation of Scd1 increased the thermogenic response of WAT in both naïve and obese status. Also, ablation of Scd1 was necessary to maintain a beige adipocyte phenotype and prohibit ADSCs from acquiring the morphology of white adipocytes. Previous studies on mice with Scd1-specific deletions in liver or skin showed that Scd1 deficiency functioned distinctly in obesity (21, 22). Such difference can be attributed to its differential roles in metabolism regulation and organ specificity. Nevertheless, suppression of Scd1 can improve metabolic stress. By employing $U^{Cre}Scd1^{flox}$, $F^{Cre}Scd1^{flox}$, and $D^{Cre}Scd1^{flox}$ mice, we conclude that Scd1 deficiency potentiates beige adipogenesis, raising a hitherto unappreciated role of Scd1 in dictating the differentiation fate of progenitor cells. With the progressions in identifying the specific marker of ADSCs, future investigations into Scd1 deficiency in preadipocytes will provide novel understanding and therapeutic targets for metabolic disorders.

Scd1 is the rate-limiting enzyme for catalyzing saturated fatty acids into monounsaturated fatty acids. When it is deficient, an accumulation of saturated fatty acids and an impairment of unsaturated fatty acids can be observed (34, 35). Our results demonstrated that replenishment of oleic acid can equilibrate the superabundant levels of succinate in Scd1-deficient ADSCs, rectifying the propensity of these cells to acquire beige adipocyte morphology and thermogenic capacity. Our findings also provide insights into the potential use of succinate to control ADSCs in the direction of beige adipocyte generation, as demonstrated through both in vitro and in vivo tracing experiments. These results corroborate a recent study that highlighted the importance of succinate in thermogenesis by directly acting on brown adipocytes (36). Also, dietary supply of succinate protected mice against HFD-induced obesity (36). These results provide the basis for illustrating a link between lipid acid metabolism and succinate in promotion of beige adipocyte generation. Yet, the regulatory mechanisms for succinate accumulation in Scd1-deficient ADSCs remain elusive. By employing the metabolic flux analysis, we found that succinate accumulation in Scd1-deficient ADSCs and their differentiated adipocytes may come from glutamate via GABA shuttle rather than from glucose. Glutamate metabolism may be an alternative pathway to drive beige adipogenesis, but its potential function and mechanisms in fighting metabolic disorders deserve further investigation.

By utilization of Atpenin A5 and OAA, the necessity of mitochondrial complex II activity in dictating ADSC fate was verified. Mitochondrial complex II is a critical enzyme that links the TCA and ETC. Previous studies have demonstrated that the ROS generated by mitochondrial complexes plays important roles in oxidative damage, as well as cell differentiation and death (37–39). Indeed, we found a high level of ROS in mitochondria from Scd1-deficient adipocytes. Their ROS generation can be induced by succinate stimulation. Improvement of substantial antioxidant capacity by mitoquinone can down-regulate the promotion of succinate in beige adipogenesis. Due to the limitation in using inhibitors to specifically block mitochondrial ROS generated from forward ETC and reverse ETC, future investigations should parse out the role of ROS in beige adipogenesis. Additionally, the highly activated AMPK signaling pathway in Scd1-deficient mice has been reported to increase fatty acid oxidation (40). However, the mechanism of Scd1 in the regulation of AMPK is unclear (41). Detailed investigations on the orchestration between fatty acid metabolism and AMPK signaling will improve our understanding of the cell fate of beige adipogenesis.

Adipose tissue is highly plastic in maintaining nutrient homeostasis. In our study, we show that lack of Scd1 can change fatty acid profiles, and subsequently dictate ADSCs with a tendency for beige adipogenesis by strengthening mitochondrial complex II activity fueled by succinate. Previous studies have reported that the expression and activity of Scd1 in mouse were related to environmental stimuli, with up-regulation in obesity status but down-regulation in cold exposure or physical exercise (42, 43). Thus, Scd1 is a sensor of metabolic changes in ADSCs. Regulation strategies on the axis of Scd1–succinate–mitochondrial complex II could direct adipogenesis and potentially fight obesity.

Materials and Methods

$Scd1^{tm1Ntam}$ mice (B6.129-$Scd1^{tm1Ntam}$/JJ, 006201), Ucp1-Cre mice [B6.FVB-Tg(Ucp1-cre)1Evdr/J, 24670], and Dermo1-Cre mice [B6.129X1-$Twist2^{tm1.1(cre)Dor}$/J, 008712] were purchased from The Jackson Laboratory. $Scd1^{ab\text{-}Xyk}$ mice (BALB/c background) were described in previous studies (44). Fabp4-Cre mice [B6.Cg-Tg(Fabp4-cre)/Nju, N000114] and mTmG reporter mice [B6.129(Cg)-$Gt(ROSA)26Sor^{tm4(ACTB\text{-}tdTomato,\text{-}EGFP)}$/Nju, N000041] were purchased from the Model Animal Research Center of Nanjing University. $Scd1^{flox}$ mice were purchased from the Shanghai Model Organisms Center. Genetically modified sex-matched littermate WT mice were used as controls. Mice were housed in the animal facilities of the Shanghai Institutes for Biological Sciences, Chinese Academy of Sciences under pathogen-free conditions. All animal experiments were approved by the Institutional Animal Care and Use Committee of the Institute of Health Sciences, Shanghai Institutes for Biological Sciences of the Chinese Academy of Sciences. Additional information on materials, experimental protocols, and statistical analyses is provided in *SI Appendix*.

Data Availability. All additional data and information are included in *SI Appendix* as figures, additional legends, references, and tables for primers.

ACKNOWLEDGMENTS. This study was supported by grants from the National Key R&D Program of China (2018YFA0107500 and 2018YFC1704300); Scientific Innovation Project of the Chinese Academy of Sciences (XDA16020403); National Natural Science of China Programs (81861138015, 31771641, 31961133024, 31601106, 81530043, and 81571612); Ministry of Foreign Affairs and International Cooperation Italy-China Science and Technology Cooperation (PGR00961); and Youth Innovation Promotion Association research fund from the Chinese Academy of Sciences. We thank Dr. Baojie Li for his support in metabolic flux analysis.

1. T. C. Walther, R. V. Farese, Jr, Lipid droplets and cellular lipid metabolism. *Annu. Rev. Biochem.* **81**, 687–714 (2012).
2. E. L. Arrese, J. L. Soulages, Insect fat body: Energy, metabolism, and regulation. *Annu. Rev. Entomol.* **55**, 207–225 (2010).
3. E. D. Rosen, B. M. Spiegelman, What we talk about when we talk about fat. *Cell* **156**, 20–44 (2014).
4. A. L. Ghaben, P. E. Scherer, Adipogenesis and metabolic health. *Nat. Rev. Mol. Cell Biol.* **20**, 242–258 (2019).
5. V. Peirce, S. Carobbio, A. Vidal-Puig, The different shades of fat. *Nature* **510**, 76–83 (2014).
6. B. Cannon, J. Nedergaard, Brown adipose tissue: Function and physiological significance. *Physiol. Rev.* **84**, 277–359 (2004).
7. C. M. Kusminski, P. E. Bickel, P. E. Scherer, Targeting adipose tissue in the treatment of obesity-associated diabetes. *Nat. Rev. Drug Discov.* **15**, 639–660 (2016).
8. M. Harms, P. Seale, Brown and beige fat: Development, function and therapeutic potential. *Nat. Med.* **19**, 1252–1263 (2013).
9. J. Wu *et al.*, Beige adipocytes are a distinct type of thermogenic fat cell in mouse and human. *Cell* **150**, 366–376 (2012).
10. I. G. Shabalina *et al.*, UCP1 in brite/beige adipose tissue mitochondria is functionally thermogenic. *Cell Rep.* **5**, 1196–1203 (2013).
11. A. Giordano, A. Frontini, S. Cinti, Convertible visceral fat as a therapeutic target to curb obesity. *Nat. Rev. Drug Discov.* **15**, 405–424 (2016).
12. P. Seale *et al.*, PRDM16 controls a brown fat/skeletal muscle switch. *Nature* **454**, 961–967 (2008).
13. Q. A. Wang, C. Tao, R. K. Gupta, P. E. Scherer, Tracking adipogenesis during white adipose tissue development, expansion and regeneration. *Nat. Med.* **19**, 1338–1344 (2013).
14. Y. H. Tseng *et al.*, New role of bone morphogenetic protein 7 in brown adipogenesis and energy expenditure. *Nature* **454**, 1000–1004 (2008).
15. T. Inagaki, J. Sakai, S. Kajimura, Transcriptional and epigenetic control of brown and beige adipose cell fate and function. *Nat. Rev. Mol. Cell Biol.* **17**, 480–495 (2016).
16. W. Wang, P. Seale, Control of brown and beige fat development. *Nat. Rev. Mol. Cell Biol.* **17**, 691–702 (2016).

17. G. Haemmerle *et al*., Defective lipolysis and altered energy metabolism in mice lacking adipose triglyceride lipase. *Science* **312**, 734–737 (2006).
18. J. S. Albert *et al*., Null mutation in hormone-sensitive lipase gene and risk of type 2 diabetes. *N. Engl. J. Med.* **370**, 2307–2315 (2014).
19. Y. Bai *et al*., X-ray structure of a mammalian stearoyl-CoA desaturase. *Nature* **524**, 252–256 (2015).
20. A. M. ALJohani, D. N. Syed, J. M. Ntambi, Insights into stearoyl-CoA desaturase-1 regulation of systemic metabolism. *Trends Endocrinol. Metab.* **28**, 831–842 (2017).
21. M. Miyazaki *et al*., Hepatic stearoyl-CoA desaturase-1 deficiency protects mice from carbohydrate-induced adiposity and hepatic steatosis. *Cell Metab.* **6**, 484–496 (2007).
22. H. Sampath *et al*., Skin-specific deletion of stearoyl-CoA desaturase-1 alters skin lipid composition and protects mice from high fat diet-induced obesity. *J. Biol. Chem.* **284**, 19961–19973 (2009).
23. Y. Lu *et al*., Scd1ab-Xyk: A new asebia allele characterized by a CCC trinucleotide insertion in exon 5 of the stearoyl-CoA desaturase 1 gene in mouse. *Mol. Genet. Genomics* **272**, 129–137 (2004).
24. C. Guerra, R. A. Koza, H. Yamashita, K. Walsh, L. P. Kozak, Emergence of brown adipocytes in white fat in mice is under genetic control. Effects on body weight and adiposity. *J. Clin. Invest.* **102**, 412–420 (1998).
25. M. Shao *et al*., Zfp423 maintains white adipocyte identity through suppression of the beige cell thermogenic gene program. *Cell Metab.* **23**, 1167–1184 (2016).
26. L. Vishvanath *et al*., Pdgfrβ+ mural preadipocytes contribute to adipocyte hyperplasia induced by high-fat-diet feeding and prolonged cold exposure in adult mice. *Cell Metab.* **23**, 350–359 (2016).
27. Y. H. Lee, A. P. Petkova, A. A. Konkar, J. G. Granneman, Cellular origins of cold-induced brown adipocytes in adult mice. *FASEB J.* **29**, 286–299 (2015).
28. M. Rosenwald, A. Perdikari, T. Rülicke, C. Wolfrum, Bi-directional interconversion of brite and white adipocytes. *Nat. Cell Biol.* **15**, 659–667 (2013).
29. M. Saraste, Oxidative phosphorylation at the fin de siècle. *Science* **283**, 1488–1493 (1999).
30. K. Shinoda *et al*., Genetic and functional characterization of clonally derived adult human brown adipocytes. *Nat. Med.* **21**, 389–394 (2015).
31. H. Xue *et al*., Molecular signatures and functional analysis of beige adipocytes induced from in vivo intra-abdominal adipocytes. *Sci. Adv.* **4**, eaar5319 (2018).
32. D. Merrick *et al*., Identification of a mesenchymal progenitor cell hierarchy in adipose tissue. *Science* **364**, eaav2501 (2019).
33. M. D. Muzumdar, B. Tasic, K. Miyamichi, L. Li, L. Luo, A global double-fluorescent Cre reporter mouse. *Genesis* **45**, 593–605 (2007).
34. M. A. Lounis, K. F. Bergeron, M. S. Burhans, J. M. Ntambi, C. Mounier, Oleate activates SREBP-1 signaling activity in *SCD1*-deficient hepatocytes. *Am. J. Physiol. Endocrinol. Metab.* **313**, E710–E720 (2017).
35. S. Ducheix *et al*., Deletion of stearoyl-CoA desaturase-1 from the intestinal epithelium promotes inflammation and tumorigenesis, reversed by dietary oleate. *Gastroenterology* **155**, 1524–1538.e9 (2018).
36. E. L. Mills *et al*., Accumulation of succinate controls activation of adipose tissue thermogenesis. *Nature* **560**, 102–106 (2018).
37. C. L. Quinlan *et al*., Mitochondrial complex II can generate reactive oxygen species at high rates in both the forward and reverse reactions. *J. Biol. Chem.* **287**, 27255–27264 (2012).
38. F. Scialò, D. J. Fernández-Ayala, A. Sanz, Role of mitochondrial reverse electron transport in ROS signaling: Potential roles in health and disease. *Front. Physiol.* **8**, 428 (2017).
39. K. V. Tormos *et al*., Mitochondrial complex III ROS regulate adipocyte differentiation. *Cell Metab.* **14**, 537–544 (2011).
40. E. Kim, J. H. Lee, J. M. Ntambi, C. K. Hyun, Inhibition of stearoyl-CoA desaturase1 activates AMPK and exhibits beneficial lipid metabolic effects in vitro. *Eur. J. Pharmacol.* **672**, 38–44 (2011).
41. P. Dobrzyn *et al*., Stearoyl-CoA desaturase 1 deficiency increases fatty acid oxidation by activating AMP-activated protein kinase in liver. *Proc. Natl. Acad. Sci. U.S.A.* **101**, 6409–6414 (2004).
42. P. Cohen *et al*., Role for stearoyl-CoA desaturase-1 in leptin-mediated weight loss. *Science* **297**, 240–243 (2002).
43. C. Peres Valgas da Silva, D. Hernández-Saavedra, J. D. White, K. I. Stanford, Cold and exercise: Therapeutic tools to activate brown adipose tissue and combat obesity. *Biology (Basel)* **8**, E9 (2019).
44. D. Feng *et al*., Stearoyl-CoA desaturase 1 deficiency protects mice from immune-mediated liver injury. *Lab. Invest.* **89**, 222–230 (2009).